Impedance Bandwidth of a Wire Dipole with the Split-Coaxial Balun

Sergey N. Makarov and Reinhold Ludwig

ECE Department
Worcester Polytechnic Institute
100 Institute Rd.
Worcester, MA 01609-2280

Email:
makarov@wpi.edu ludwig@wpi.edu

Draft

July 22nd 2006

Abstract

The half-wave wire dipole with a split-coaxial balance-to-unbalance (balun) transformation is a classic antenna configuration that so far has been treated mostly qualitatively. In this study, an analytical TL model of the balun network is proposed that gives a simple closed-form expression for the termination impedance of the antenna. The model is based on the coupled transmission line approach; it accepts the impedance of a center-fed dipole as input parameter. The transmission line approach is validated by full wave simulations and enables us to establish quantitative estimates for the expected impedance bandwidth of the network consisting of the dipole, balun, and a non-splitted coaxial line of fixed length. These estimates suggest a 12% bandwidth for the resonant dipole-balun configuration and a greater than 20% bandwidth for the combined dipole, balun and non-splitted line configuration. The analytical model and numerical simulations are confirmed by measurement results.

Introduction

Conventional baluns for symmetric wire dipole antennas are reviewed in several scholar sources - see for example [1]-[5]. Our attention is concentrated on the split-tube or split-coaxial balun (a "split coax" balun in Fig. 5-42 of Ref. [4] or type 10a balun in Fig. 43-24 of Ref. [5]). The balun is to be connected to an unfolded straight-wire dipole. This balun, in contrast to some other balun types, has a very convenient conformal geometry; it is easy to manufacture with commercial off-the-shelf tubing. It may be used for spacecraft communications systems [6]. The balun itself is shown in Fig. 1, together with appropriate dimensions. Two dipole currents should exactly cancel each other on the outer conductor surface of the coaxial line after the split point, due to anticipated excitation symmetry [2]. On the other hand, the antenna is not shorted at the dipole feeding point due to the $\lambda/4$ short-to-open circuit transformation. According to [5], this type of balun "will give almost perfect balance over a wide frequency range if the slot width is kept small and symmetry is maintained at the strap end." In particular, Ref. [6] reports on an 8% bandwidth for the split-coaxial balun supporting the dipole with a reflector.

A non-conformal variation of the split-coaxial balun is known as the quarter-wave balun [1], [2], [8], that is referred to as a "$\lambda/4$ coaxial balun 1:1" in Ref. [1] - Fig. 9.25c, and as a "folded balun" in Ref. [2] - Fig. 5-26. For the quarter-wave balun, the slots are missing, but one wing of the dipole, which is connected to the inner conductor of the coaxial line, is simultaneously connected to the outer conductor at the distance of $\lambda/4$ from the feed by a straight rod. It is stated in [2] that this balun is "of course, not broadband because of the quarter wavelength involved in its construction". Ground plane may be present [8] or not [1], [2] at a distance of $\lambda/4$ from the feed. Yet another variation is a three-wire balun [5], [8] that completely replaces the $\lambda/4$ section of the coaxial line by three wires, two of which are connected to the ground plane at $\lambda/4$ and one - to the inner conductor of the coaxial feed at the same distance.

Fig. 1 suggests that quantitative theory of the split-coaxial balun may be based on the three-conductor transmission line model. Such a model has been discussed independently in two papers [8], [9]. In both references, three independent conductors and a separate ground have been considered, which initially leads to a six-port transmission line network with the associated static capacitance matrix [8]. Though a general expression for the antenna admittance has been obtained in [8] and [9], it was not quantified in terms of the parameters of the balun such as slot length, width, and thickness.

The three-conductor transmission line with no extra ground may be also described in terms of two independent propagating modes. Collin [11] first described two modes that can propagate along the split-coaxial line; one of them is the perturbed TEM fundamental mode (coaxial or bifilar mode according to terminology used in [12],[13]) and another is the slot mode that also extends into the surrounding space (monofilar mode according to the same references). This analysis, and an analysis reported in [14], was performed for the infinitely thin coaxial tubes only. On the other hand, Milligan [4] classified the two modes in the splitted line as TEM and TE_{11}; the latter notation is somewhat questionable due to anticipated cutoff of the coaxial TE_{11} mode.

Despite a significant amount of research efforts on the split-coaxial balun outlined above, two fundamental questions remain unanswered. First, there is no simple quantitative estimate of the impedance bandwidth of the half-wave dipole with the split-coaxial balun versus the bandwidth of the equivalent center-fed dipole. Second, impedance matching and broadbanding properties of the split-coaxial balun loaded with the wire dipole have not yet been investigated quantitatively. Note that return loss improvement provided by the matching/balun network to the dipole antenna(s) may be significant [7].

Our approach to the split-coaxial balun is based on separation of the balun into two coupled symmetric transmission lines. Coupled transmission line theory - see [10], [15]-[19] - introduces even and odd modes of propagation; with the even mode being independent of the mutual coupling parameters. For the symmetric case of a two-line network, the transmission equations for even and odd modes are decoupled, and every

mode is described by the familiar two-port network equation and has its own characteristic impedance [15], [17]-[19]. Such an approach will lead to a simple closed-form solution for the transformed antenna impedance, which appears to be in excellent agreement with the full-wave simulations and experiment. The analytical solution allows us to rapidly estimate and optimize dipole performance over a wide range of balun parameters.

This paper is organized as follows: Section I describes the line and the load model, and the impedance transformation results. Section II discusses bandwidth of the half-wave dipole with a quarter-wave split-coaxial transformer. Section III gives a method of bandwidth enhancement, using two closely spaced resonances. Section IV presents the corresponding experimental results and Section V concludes the paper.

I. Coupled transmission line model of the balun

1.1. Separation into two coupled lines

In Fig. 2 we suggest a way of separating the splitted coaxial line into two coupled symmetric transmission lines TL1 and TL2. The central conductor plays the role of ground common to both lines. This designation of "ground" has no special relevance beyond the fact that it is a convenient reference designation for maintaining symmetry. Two coupled lines are characterized by static self-capacitances C_{11} and C_{22}, and mutual capacitance C_{12} schematically shown in Fig. 2 - bottom. The following assumptions are made that are based on the physical dimensions for the manufactured dipoles - see Fig. 1:

i. the coaxial tube has a significant thickness $c-b$ so that the slot width is smaller than or equal to this value: $d \le c-b$;
ii. slot width d is small compared to the inner radius of coaxial tube b;
iii. radius of the inner rod a is on the order of the inner radius of the coaxial tube b; in other words, the inner conductor is considered "thick".

Following these assumptions, the self-capacitances C_{11} and C_{22} are approximately equal to half of the static capacitance of the non-slotted coaxial line each [10]. Mutual

capacitance C_{12} is that of two narrow slots (dominant part) plus the capacitance between two curved conductors (secondary contribution). Each of the slots is modeled by a parallel-plate capacitor. The same model is applied to the curved conductors. They are replaced by parallel plates of the same projection area 2*b*, with an effective separation distance b_{eff}. One thus has

$$C_{11} \approx \pi \frac{\varepsilon_0}{\ln(b/a)}, \quad C_{22} \approx \pi \frac{\varepsilon_0}{\ln(b/a)}, \quad C_{12} \approx 2\frac{\varepsilon_0 (c-b)}{d} + \frac{\varepsilon_0 2b}{b_{\text{eff}}} \tag{1}$$

where ε_0 is the dielectric constant of vacuum for the air-filled line. We have chosen the effective separation distance to be $b_{\text{eff}} = 0.5b$. It is evident that the capacitance expressions in Eq. (1) represent simple approximations that can to be replaced by more accurate static capacitance expressions if desired. The implication of Eq. (1) suggests that the slot mode described in the introduction mostly concentrates within the slot and less in the surrounding space.

1.2. Coupled symmetric transmission line model

Fig. 3 shows the coupled TL model that utilizes the capacitance values established above. The characteristic inductances for the air-filled coupled line are given by [18]

$$L_{11}C_{11} = \mu_0\varepsilon_0, \quad L_{22}C_{22} = \mu_0\varepsilon_0, \quad L_{12} = L_{11}\frac{C_{11}}{C_{12}+C_{22}} \tag{2}$$

where μ_0 is magnetic permeability of vacuum. The characteristic impedances and propagation constants for the even (equal line voltages) and odd (opposite line voltages) modes read [10],[18],[19]

$$Z_e = \frac{1}{c_0 C_{11}} = \frac{1}{c_0 C_{22}}, \quad Z_o = \frac{1}{c_0 C_0} = \frac{1}{c_0 (C_{11}+2C_{12})}, \quad \gamma_o = \gamma_e = \gamma_0 = jk_0 \tag{3}$$

With reference to Fig. 3, one obtains the chain, or ABCD matrixes, for the even and odd mode of the coupled line of length l in the form [15]

$$\begin{bmatrix} \frac{1}{2}(V_1+V_2) \\ \frac{1}{2}(I_1+I_2) \end{bmatrix} = A_e \cdot \begin{bmatrix} \frac{1}{2}(V_3+V_4) \\ -\frac{1}{2}(I_3+I_4) \end{bmatrix}, \quad A_e = \begin{bmatrix} \cos k_0 l & jZ_e \sin k_0 l \\ j/Z_e \sin k_0 l & \cos k_0 l \end{bmatrix} \tag{4}$$

$$\begin{bmatrix} \frac{1}{2}(V_1-V_2) \\ \frac{1}{2}(I_1-I_2) \end{bmatrix} = A_o \cdot \begin{bmatrix} \frac{1}{2}(V_4-V_3) \\ -\frac{1}{2}(I_3-I_4) \end{bmatrix}, \quad A_o = \begin{bmatrix} \cos k_0 l & jZ_o \sin k_0 l \\ j/Z_o \sin k_0 l & \cos k_0 l \end{bmatrix} \tag{5}$$

where $V_{1,2,3,4}$ are termination voltages and $I_{1,2,3,4}$ are termination currents. Both matrixes A_e and A_o are equivalent to the ABCD matrix for a single transmission line with the corresponding characteristic impedances Z_e and Z_o, respectively.

1.3. Termination

Fig. 4a shows the termination setup for the dipole, balun, and the continued coaxial line. TL1 is shorted at the input - one dipole wing shorts this line. TL2 is connected to the equivalent antenna circuit - an ideal voltage source in series with the dipole (self) impedance Z_D. On the opposite end, two line conductors are connected in shunt at l (since the slot disappears) and form the outer conductor of a continued coaxial line. Ground (center conductor of the coupled line) becomes the inner conductor of the continued coaxial line.

The arrangement shown in Fig. 4a allows us to establish the *S*-parameters of the balun [20], [21] and the related complex antenna factor (CAF) [21], or the reciprocal antenna transfer function. This step is necessary when the phase distortion characteristics of the dipole are evaluated as a function of frequency. In the present study, we are only interested in the impedance transformation of the split-coaxial balun. Therefore, the equivalent circuit has the form shown in Fig. 4b. It includes the dipole with impedance

Z_D connected to a balun of length l and a non-splitted coaxial TL section of length L. The transformed impedance is given by

$$Z_s = \frac{V_s}{I_s} \tag{6}$$

where V_s is a voltage source applied to the terminals of the transmission line and I_s is the computed current. Calculations are based on chain matrixes (4) and (5), and are given in the next subsection.

1.4. Transformed antenna impedance

With reference to Fig. 4b, the chain matrix for the transmission line section of length L yields

$$\begin{bmatrix} V_{\text{coax}} \\ -I_{\text{coax}} \end{bmatrix} = A_{\text{coax}} \cdot \begin{bmatrix} V_s \\ -I_s \end{bmatrix}, \quad A_{\text{coax}} = \begin{bmatrix} \cos k_0 L & jZ_{\text{coax}} \sin k_0 L \\ j/Z_{\text{coax}} \sin k_0 L & \cos k_0 L \end{bmatrix} \tag{7}$$

where Z_{coax} is the characteristic impedance of the non-splitted line. The termination conditions on the antenna side and on the opposite side read

$$V_1 = 0, \quad V_2 = -Z_D I_2, \quad V_3 = V_4 = -V_{\text{coax}}, \quad I_3 + I_4 = I_{\text{coax}} \tag{8}$$

in terms of termination voltages $V_{1,2,3,4}$ and termination currents $I_{1,2,3,4}$.

Substitution of Eq. (8) into Eq. (4) for the even mode and using Eq. (7) gives

$$\begin{bmatrix} -\frac{1}{2} Z_D I_2 \\ \frac{1}{2}(I_1 + I_2) \end{bmatrix} = A_e \cdot \begin{bmatrix} -V_{\text{coax}} \\ +\frac{1}{2} I_{\text{coax}} \end{bmatrix} = A_e \cdot \begin{bmatrix} -1 & 0 \\ 0 & -1/2 \end{bmatrix} \begin{bmatrix} V_{\text{coax}} \\ -I_{\text{coax}} \end{bmatrix} = A_e \times \begin{bmatrix} -1 & 0 \\ 0 & -1/2 \end{bmatrix} \times A_{\text{coax}} \begin{bmatrix} V_{\text{s}} \\ -I_{\text{s}} \end{bmatrix}$$

(9)

Substitution of Eq. (8) into Eq. (5) for the odd mode allows us to find a relation between I_1 and I_2

$$\begin{bmatrix} +\frac{1}{2}Z_D I_2 \\ \frac{1}{2}(I_1 - I_2) \end{bmatrix} = A_o \cdot \begin{bmatrix} 0 \\ -\frac{1}{2}(I_3 - I_4) \end{bmatrix} \Rightarrow A_o^{-1} \cdot \begin{bmatrix} +\frac{1}{2}Z_D I_2 \\ \frac{1}{2}(I_1 - I_2) \end{bmatrix} = \begin{bmatrix} 0 \\ -\frac{1}{2}(I_3 - I_4) \end{bmatrix} \Rightarrow$$

$$\left[+\frac{1}{2}Z_D I_2 \right] a_{o\ 11}^{-1} + \left[\frac{1}{2}(I_1 - I_2) \right] a_{o\ 12}^{-1} = 0 \Rightarrow I_1 = (1+K) I_2, \quad K = -\frac{Z_D a_{o\ 11}^{-1}}{a_{o\ 12}^{-1}} \tag{10}$$

Substitution of this relation into Eq. (9) will express the termination current I_s in terms of the termination voltage V_s as follows

$$\begin{bmatrix} -Z_D I_2 \\ (2+K) I_2 \end{bmatrix} = \underbrace{A_e \times \begin{bmatrix} -2 & 0 \\ 0 & -1 \end{bmatrix} \times A_{\text{coax}}}_{M} \cdot \begin{bmatrix} V_s \\ -I_s \end{bmatrix} = \begin{bmatrix} m_{11} V_s - m_{12} I_s \\ m_{21} V_s - m_{22} I_s \end{bmatrix} \Rightarrow$$

$$(2+K) m_{11} V_s - (2+K) m_{12} I_s + Z_D m_{21} V_s - Z_D m_{22} I_s = 0 \Rightarrow V_s = \frac{(2+K) m_{12} + Z_D m_{22}}{(2+K) m_{11} + Z_D m_{21}} I_s \tag{11}$$

Thus, the impedance Z_s is finally given by

$$Z_s = \frac{(2+K) m_{12} + Z_D m_{22}}{(2+K) m_{11} + Z_D m_{21}}, \quad M = \begin{bmatrix} \cos k_0 l & j Z_e \sin k_0 l \\ j / Z_e \sin k_0 l & \cos k_0 l \end{bmatrix} \begin{bmatrix} -2\cos k_0 L & -2 j Z_{\text{coax}} \sin k_0 L \\ j / Z_{\text{coax}} \sin k_0 L & \cos k_0 L \end{bmatrix} \tag{12a}$$

where

$$K = -\frac{Z_D a_{o\ 11}^{-1}}{a_{o\ 12}^{-1}}, \quad A_o^{-1} = \begin{bmatrix} \cos k_0 l & -j Z_o \sin k_0 l \\ -j / Z_o \sin k_0 l & \cos k_0 l \end{bmatrix}, \quad K = -j \frac{Z_D}{Z_o} \cot(k_0 l) \tag{12b}$$

If the balun is exactly a quarter wavelength ($K = 0$) and the additional coaxial line section of length L is absent, the termination impedance becomes that for the familiar quarter-wavelength transformer [8]

$$Z_s = \frac{Z_e Z_e}{Z_D} \tag{13}$$

For a coaxial line with $Z_{\text{coax}} = 50\Omega$, one find $Z_e \approx 100\Omega$. Therefore, the split-coaxial balun will indeed behave as a 4:1 transformer for an idealized antenna load of $Z_D = 50\Omega$. Unfortunately, the load is now not properly matched. In order to achieve matching to a 50Ω, the characteristic impedance of the base non-splitted coaxial line should be considerably decreased.

It is interesting to note that for the folded dipole, whose input impedance is approximately four times the dipole impedance ([1], pp.516-517), Eq. (13) would give an almost ideal match to the balun section of the coaxial line with $Z_{\text{coax}} = 50\Omega$. Our attention is, however, concentrated on the unfolded dipole.

1.5. Comparison with full-wave simulations (412 MHz dipole)

In order to compare the results with a full-wave simulation software (ANSOFT HFSS v. 10.1) the following steps are done: First, the impedance Z_D of a center-fed dipole of interest is found numerically in ANSOFT and then tabulated. This impedance is then substituted in Eqs. (12) and the termination impedance Z_s is evaluated over a desired frequency band.

Simultaneously, another ANSOFT project is created that includes the same dipole, balun connection, balun itself, and the additional coaxial line section of length L The coaxial line is fed from the opposite end using a lumped port that defines the TEM E-field across the cross-sectional ring of the coaxial line. Fine meshes with about 100,000 tetrahedra and a discrete frequency sweep are used to obtain accurate results.

Table 1 gives the physical parameters of a UHF dipole and a balun used for comparison. Both the slot and the dipole wings have the length of 170 mm, which approximately corresponds to the center frequency of 412 MHz. For convenience, here and in what follows we use standard off-the-shelf brass tubing/rod sizes available from McMaster Carr. The characteristic impedance of the non splitted coaxial line is still chosen to be as close as possible to $Z_{\text{coax}} = 50\Omega$. In that case Z_e is close to 100Ω and the split-coaxial balun is not expected to be matched properly, as discussed in the previous section.

Fig. 5 shows the surface current density distribution (logarithmic scale) for a dipole with the split-coaxial balun (left) and for the unbalanced dipole with the same parameters - right. Parameters for both dipoles are listed in Table 1. For the dipole with balun, the current density on the outer conductor beyond the balun is at least 120-140 times smaller than the maximum current density on the dipole wings. This value multiplied with the ratio of the radii gives us the ratio of the total currents inside and outside the coaxial line as at least 40. Thus, the balun performs its major function: the current cancellation on the outer side of the coaxial line. Without the balun (Fig. 5 -right) the ratio of total currents reduces to approximately 3. The mode on the outer side of the conductor for the unbalanced dipole is a leaky traveling wave that may propagate along a single metal conductor (Sommerfeld wave) - see [22] and [1], pp. 549-555 - and be reflected from the terminations. Therefore, one can see a well-developed standing wave pattern - see Fig. 5 - right.

Fig. 6a) shows impedance of the center-fed test dipole with 170 mm wing length. Fig. 6b gives the impedance of the same dipole but connected to the balun and a continued coaxial line with the characteristic impedance of 54 Ω - see Table 1. The resistance is shown by a solid curve and the reactance is depicted by a dashed curve. One can see that there is no impedance matching in the present case and multiple resonances do occur. The corresponding return loss is shown in Fig. 6c) and d). All these solutions have been found using ANSOFT HFSS. The corresponding result of the transmission line theory (Eqs. (12)) with the parameters listed in Table 1 is given by the thin-lined curves in Fig. 6b) and 6d), respectively. The agreement between the two solutions appears nearly

excellent, especially in Fig. 6b) where these solutions almost coincide, despite a complicated multi-resonant behavior of the non-matched balun.

II. Resonant impedance bandwidth

2.1. Balun parameters

In order to match the split-coaxial balun to the dipole and to the 50 Ω front-end termination network, the following steps are done: First, the impedance Z_D of a center-fed dipole is again found numerically via ANSOFT HFSS and then tabulated. The resonant frequency and the resonant dipole wavelength $\lambda_{D\mathrm{res}}$ are found from the condition $\mathrm{Im}(Z_D) = 0$. The slot length l is defined as $\lambda_{D\mathrm{res}}/4$. The length of the additional transmission line section *L* is kept at a minimum, which is necessary to ensure mechanical stability of the antenna - we choose $L = 10\mathrm{mm}$.

To match the dipole resonant resistance, the even-mode impedance is found from Eqs. (1) and (2). Specifically, we have

$$Z_e = \frac{\ln(b/a)}{c_0 \pi \varepsilon_0} \tag{14}$$

At the same time, Eq. (13) needs to be satisfied based on $Z_s = 50\Omega$, which gives

$$\frac{b}{a} = \exp(c_0 \pi \varepsilon_0 \sqrt{50 Z_{Dres}}) \tag{15}$$

where Z_{Dres} is the dipole resistance at resonance. Either *a* or *b* in Eq. (15) can be varied so as to achieve impedance matching. We prefer to vary *a* - the radius of the inner conductor. All other parameters remain fixed as specified in the previous section (Table 1); only the dipole wing length is changed from 170 mm to 156 mm compared to the previous case. The dipole is now centered at about 440 MHz. Table 2 provides with the

parameters of the balun that most closely satisfy the conditions listed above for standard brass tubing/rod sizes.

2.2. Resonant antenna bandwidth (440 MHz dipole)

Fig. 7a) shows the return loss of the center-fed dipole with 156 mm wing length and Fig. 7b) gives the return loss of the dipole with the balun designed according to Table 2. The thick curve corresponds to the ANSOFT HFSS solution whereas the thin curve is the transmission line model. The agreement between both solutions is good.

The main observation is that the bandwidth of the dipole with the splitted-coaxial balun is about 12% in Fig. 7b). This is larger than the bandwidth of the original center-fed dipole (i.e., 8%) by approximately a factor of 1.4. To explain this result we consider Eqs. (12) with *L* equal to zero. This yields

$$Z_s = \frac{(2+K)\,jZ_e \sin k_0 l + Z_D \cos k_0 l}{(2+K)2\cos k_0 l + 2Z_D\, j / Z_e \sin k_0 l}, \quad K = -j\frac{Z_D}{Z_o}\frac{\cos k_0 l}{\sin k_0 l} \tag{16}$$

An asymptotic expansion with the following approximations

$$k_0 l = \frac{\pi}{2} + \delta, \quad \delta << 1, \quad \cos k_0 l \approx -\delta, \quad \sin k_0 l \approx 1 - \delta^2/2, \quad K \approx j\frac{Z_D}{Z_o}\delta \tag{17}$$

results, to main order of approximation, in the expression

$$Z_s \approx \frac{(2+K)\,jZ_e - Z_D\delta}{-2(2+K)\delta + 2Z_D\, j / Z_e} \approx \frac{2Z_e + j\delta Z_D\left(\frac{Z_e}{Z_o}+1\right)}{2Z_D / Z_e + j4\delta} \approx \frac{Z_e^2}{Z_D}\left(1 + \left[\, j\delta\left(\frac{Z_D}{2Z_o} + \frac{Z_D}{2Z_e} - 2\frac{Z_e}{Z_D}\right)\right]\right) \tag{18}$$

For the dipole from Table 2, the reactance term in the square brackets in Eq. (18) is reasonably small and positive; so is the dipole reactance close to the resonance. One may therefore conclude that it is a better matching of $\mathrm{Re}\left(Z_e Z_e / Z_{Dres}\right)$ to 50Ω than matching of the original Z_{Dres} to 50Ω, which makes the bandwidth wider. In other words, the

bandwidth increase for the resonant dipole with the split-coaxial balun is a familiar action of the quarter wavelength transformer on real impedances.

2.3. Effect of uncertainty in slot width

An important question from the viewpoint of hardware prototyping is the effect of inaccuracy in slot width. Fig. 7c) investigates the effect of varying the slot width from 1 to 2 mm and its behavior on the return loss obtained with the transmission line model. Ten curves that correspond to different slot widths between 1 and 2 mm almost coincide. Therefore, the inaccuracy in slot cutting has generally a minor influence on the antenna performance. Similar results have been obtained with ANSOFT HFSS.

2.4. Effect of varying slot length

Fig. 7d) shows the effect of varying the slot length about $\lambda_{Dres}/4$ by $\pm 10\%$ and its effect on the return loss; the thick curve corresponds to $\lambda_{Dres}/4+10\%$. One can see that the impedance bandwidth slightly increases (up to 15%) with increasing slot length above $\lambda_{Dres}/4$. Unfortunately, Eq. (18) is unable to describe this effect, which is on the second order of magnitude with regard to the small parameter δ in Eq. (17).

III. Bandwidth enhancement

3.1. Two closely spaced resonances

With the help of the transmission line model, it has been found that the bandwidth of the dipole with balun can further be improved using the method of two closely spaced resonances. One of them is the original dipole resonance at a lower frequency. Another is a resonance of the system that consists of the balun connected to a finite, but still relatively short, section *L* of the non-splitted coaxial line with the impedance different from 50Ω. This line always presents in the hardware prototype in order to ensure mechanical stability - see Fig. 1. It is therefore advisable to use this "free" network element for bandwidth enhancement.

3.2. Bandwidth of the dipole network with two closely spaced resonances

The system balun+non-splitted line operates as a distributed matching network/filter, presumably of the second order. It may be properly tuned to achieve the second resonance at a slightly higher frequency. The dipole wing length is now 152 mm, which will correspond to the center frequency of the composite band of approximately 460 MHz. This center frequency is our final goal. Fig. 8 shows typical analytical tuning results for the return loss of the complete network (dipole+balun+non-splitted line). These results involve two parameters: balun length l that varies from 150 to 188mm in 20 steps; and non-splitted line length L that attains the values of 10, 25, 50, and 75 mm. The development of the second resonance can be seen while the non-splitted line length increases. The largest impedance bandwidth is thus obtained with $l = 174\text{mm}, l = 50\text{mm}$ as seen in Fig. 8c). It is slightly higher than 20%. However, the return loss now has a maximum in the middle of the band that is approaching -11 dB. The corresponding full wave simulation is very close to this result but reduces the maximum of the return loss within the band to approximately -13 dB.

3.3. Effect of shift of the center conductor

A slight asymmetry in the position of the center conductor of the splitted transmission line may severely degrade performance of the matching network with the dual resonances. For a shift of 0.5mm from the center position, the corresponding ANSOFT HFSS simulation predicts increase in the return from -13 dB to -8 dB in the center of the band. Therefore, in contrast to the other dipole parameters tested above, the position of the center conductor needs to be controlled rather precisely.

IV. Measurement results

4.1. Dipole prototypes (460 MHz center frequency)

Using the matching network with dual resonances, a series of UHF dipole prototypes was custom built and tested for the center frequency of the band equal to 460 MHz. The corresponding physical parameters are listed in Table 3. The prototypes are shown in Fig. 9. One outer and two inner Teflon rings, with the height of 10mm each, have been used to provide system stability and to properly position the inner conductor of the slotted

transmission line. An SMA connector is soldered to the non-splitted section of the brass transmission line at the feeding point. All other connections are made in a solderless way. The dipole prototypes are low-cost and are built with commercial off-the-shelf brass/Teflon tubing and brass rods - see Table 3. The prototypes may be assembled into an array of dipoles. All prototypes passed the "drop off" test. The dipole prototypes are intended for the use in an indoor geolocation wireless link.

4.2. Measurement results

Measurement results for the return loss of eight dipole prototypes are obtained with Agilent's 8722ET Network Analyzer and are given in Fig. 10 (thin curves) compared to the analytical model - Eqs. (12) - thick dashed curve. The agreement in the impedance bandwidth of the antenna (frequency band where return loss is less than -10 dB) is nearly excellent between the individual dipoles as well as between the measured and predicted values. The analytical network model also agrees well with the ANSOFT simulations, see Fig. 11. The ANSOFT model takes into account some fine antenna details such as feed assembly, construction nuts, inner/outer Teflon rings, etc. The measured impedance bandwidth for individual dipoles ranges from 23% to 26%.

However, within the band, the measured return loss of the individual dipoles indicates a rather random behavior, with the maximum return loss as high as -12 to -11 dB for a couple of dipole prototypes. This behavior is likely due to mechanical intolerances of the present prototypes such as a small error in the position of the center conductor, a slight asymmetry of the feed assembly, etc. Another experimental design (with closer resonances) may indeed have a better return loss within the band, but at the expense of decreasing the overall 10 dB bandwidth.

In order to reduce the effect of manufacturing intolerances, each dipole has been equipped with a thin sliding brass ring that is seen in Fig. 9. The brass ring allows us to cover a small portion of the slots (reduce the slot length) and thus change the balance between two resonances in Fig. 8. The latter circumstance allows us to adjusts (decrease) the maximum value of the return loss within the band.

A less important but still visible point of concern is a disagreement between theoretical (both the lumped circuit model and the full wave model) and experimental results in the lower UHF band at approximately 300 MHz in Fig. 10. It is believed that the experimentally observed RF leakage in Fig. 10 is due to limited bandwidth (limited to approximately 400 MHz) of the absorber material used in the present measurements and the associated antenna loading.

V. Conclusions

In this study we have presented and validated a simple closed-form analytical TL model of the wire dipole with the split-coaxial balun. The model accepts the input impedance of the center-fed dipole as an input parameter and outputs the antenna termination impedance or the antenna transfer function. The model indicated a very good agreement with the full-wave simulations obtained at three different center frequencies (412, 440, and 460 MHz) and for different geometry parameters (non-matched balun, matched resonant balun, and matched balun with two closely spaced resonances).

The model predicts the impedance bandwidth of 12% for the $\lambda/4$ resonant balun and the bandwidth in excess of 20% for the properly tuned complete antenna network (dipole+balun+supporting section of the non-splitted transmission line). UHF wire dipoles built in accordance with this model are compact and low-cost, and indicate good repeatability in the center frequency and in the impedance bandwidth; they exhibit good agreement with theoretical predictions. The measured impedance bandwidth of the UHF dipoles is approximately 23-26%. However, the return loss behavior within the band needs to be improved and controlled more precisely, by improving hardware tolerances.

The present model is equally applicable to other dipole-like antennas of interest: a broadband (bowtie) dipole, a droopy dipole intended for better azimuthal coverage, or to a quasi-folded assembly of two crossed dipoles intended for circular polarization [23]. For those systems, only the input impedance of an equivalent center-fed antenna needs to be recalculated.

References

[1] C. A. Balanis, *Antenna Theory. Analysis and Design*, Wiley, New York, 2005, third ed., pp. 538-542.

[2] W. L. Stutzman and G. A. Thiele, *Antenna Theory and Design*, Wiley, New York, 1998, second ed., pp. 183-187.

[3] R. A. Burberry, *VHF and UHF Antennas*, Peter Peregrinus Ltd., London, 1992, pp. 242-245.

[4] T. A. Milligan, *Modern Antenna Design*, Wiley-IEEE Press, New York, 2005, second ed., pp. 255.

[5] R. C. Johnson, Ed., *Antenna Engineering Handbook*, McGraw Hill, New York, 1993, third ed., pp. 43-23 - 43-27.

[6] M. S. Gatti and D. J. Nybakken, "A circularly polarized crossed drooping dipole antenna," *IEEE AP-S International Symposium*, May 1990, vol. 1, pp. 254-257.

[7] R. K. Zimmerman, "Crossed dipoles fed with a turnstile network," *IEEE Trans. Microwave Theory Techniques*, vol. 46, no. 12, Dec. 1998, pp. 2151-2156.

[8] M. du Plessis and J. H. Cloete, "Analysis of three-conductor baluns using the static capacitance matrix," *IEEE AP-S International Symposium*, May 1990, vol. 1, pp. 549-552.

[9] H. Kogo, "Analysis of split coaxial line type balun," *IEEE Trans. Microwave Theory Techniques*, vol. 8, March. 1960, pp. 245-246.

[10] D. M. Pozar, *Microwave Engineering*, Wiley, New Your, 2005, third ed.

[11] R. E. Collin, "The characteristic impedance of a slotted coaxial line," *IRE Trans. Microwave Theory Techniques*, Jan. 1956, pp. 4-8.

[12] P. P. Delonge and A. A. Laloux, "Theory of the slotted coaxial cable," *IEEE Trans. Microwave Theory Tech.*, vol. MTT-28, no. 10, Oct. 1980, pp. 1102 – 1107.

[13] D. H. Kim and H. J. Eom, "Mode matching analysis of axially slotted coaxial cable," *IEEE Antennas and Wireless Propagation Letters*, vol. 4, 2005, pp. 169-171.

[14] J. Smolarska, "Characteristic impedances of the slotted coaxial line," *IRE Trans. Microwave Theory Techniques*, April 1958, pp. 161-166.

[15] G. I. Zysman and A.K. Johnson, “Coupled transmission line networks in an inhomogeneous dielectric medium,” *IEEE Trans. Microwave Theory Tech.*, vol. MTT-17, no. 10, Oct. 1969, pp. 753 – 759.

[16] V. K. Tripathi, “Asymmetric coupled transmission lines in an inhomogeneous medium,” *IEEE Trans. Microwave Theory Tech.*, vol. MTT-23, no. 9, Sep. 1975, pp. 734 – 739.

[17] B. Bhat and S. K. Koul, *Stripline-Like Transmission Lines for Microwave Integrated Circuits*, Wiley, New York, 1989.

[18] O. Zinke und H. B. Brunswig, *Hochfrequenz Technik* I, 5 Auflage, Springer, Berlin, 1995, pp. 194-200.

[19] R. E. Collin, *Foundations for Microwave Engineering*, IEEE Press, Piscataway, NJ, 2001, second ed.

[20] T. Iwasaki and K. Tomizawa, "Measurement of S-parameters of balun and its application to determination of complex antenna factor," *2003 IEEE International Symposium on Electromagnetic Compatibility EMC '03*, May 2003, vol. 1, pp. 62-65.

[21] T. Iwasaki and K. Tomizawa, "Systematic uncertainties of the complex antenna factor of a dipole antenna as determined by two methods," *IEEE Trans. Electromagnetic Compatibility,* vol. 46, no. 2, May 2004, pp. 234-245.

[22] A. Sommerfeld, Electrodynamics, Academic Press, New York, 1952, pp. 177-190.

[23] K. Maamria and T. Nakamura, "Simple antenna for circular polarization," *IEE Proceedings on Microwaves, Antennas and Propagation*, vol. 139, no. 2, April 1992, pp. 157-158.

Tables

Table 1. Physical parameters of the dipole and the balun - non-matched balun. Characteristic impedances of the coupled line are $Z_e = 108\Omega, Z_o = 24\Omega$; characteristic impedance of the non splitted coaxial line is $Z_{\text{coax}} = 54\Omega$.

Component	Outer D (2*c*)	Inner D (2*b*)	Total length ($l + L$)	Vendor part # (McMaster Carr)
Outer coaxial tube	7/16" 11.1 mm	0.3075" 7.81mm	24" 609.6 mm	#8950K68
Inner rod	1/8" 3.2 mm	--	24" 609.6 mm	#8953K41
Free length of single dipole wing, *D*	1/8" 3.2 mm	--	6.69" 170 mm	#8953K41
Slot length from top, *l*	--	--	6.69" 170 mm	--
Slot width, *d*	--	--	59 mils 1.5 mm	--
Dipole offset from top, Δ	--	--	0.24" 6 mm	--

Table 2. Physical parameters of the dipole and the resonant λ/4 balun. Characteristic impedances of the coupled line are $Z_e = 59\Omega, Z_o = 22.5\Omega$; characteristic impedance of the non splitted coaxial line is $Z_{\text{coax}} = 29.6\Omega$.

Part	Outer D (2*c*)	Inner D (2*b*)	Total length ($l + L$)	Vendor part # (McMaster Carr)
Outer coaxial tube	7/16" 11.1 mm	0.3075" 7.81mm	7.02" 178 mm	#8950K68
Inner rod	3/16" 4.8 mm	--	8.98" 228 mm	#8859K155
Free length of single dipole wing, *D*	1/8" 3.2 mm	--	6.14" 156 mm	#8953K41
Slot length from top, *l*	--	--	6.61" 168 mm	--
Slot width, *d*	--	--	40-60 mils 1.0-1.5 mm	--
Dipole offset from top, Δ	--	--	0.24" 6 mm	--

Table 3. Physical parameters of the dipole and the balun optimized for a wider bandwidth. Characteristic impedances of the coupled line are $Z_e = 59\Omega, Z_o = 22.5\Omega$; characteristic impedance of the non splitted coaxial line is $Z_{\text{coax}} = 29.6\Omega$.

Component	Outer D ($2c$)	Inner D ($2b$)	Total length ($l + L$)	Vendor part # (McMaster Carr)
Outer coaxial tube	7/16" 11.1 mm	0.3075" 7.81mm	9.06" 230 mm	#8950K68
Inner rod	3/16" 4.76 mm	--	9.06" 230 mm	#8859K155
Free length of single dipole wing, D	1/8" 3.175 mm	--	5.98" 152 mm	#8953K41
Slot length from top, l	--	--	7.09" 180 mm	--
Slot width, d	--	--	47 mil 1.2mm	--
Dipole offset from top, Δ	--	--	0.24" 6 mm	--
Teflon PTFE tube-inner	5/16"	3/16"	Two rings: 10mm height	#8547K24
Teflon PTFE tube-outer	9/16"	7/16"	One ring: 10 mm height	#5033K36

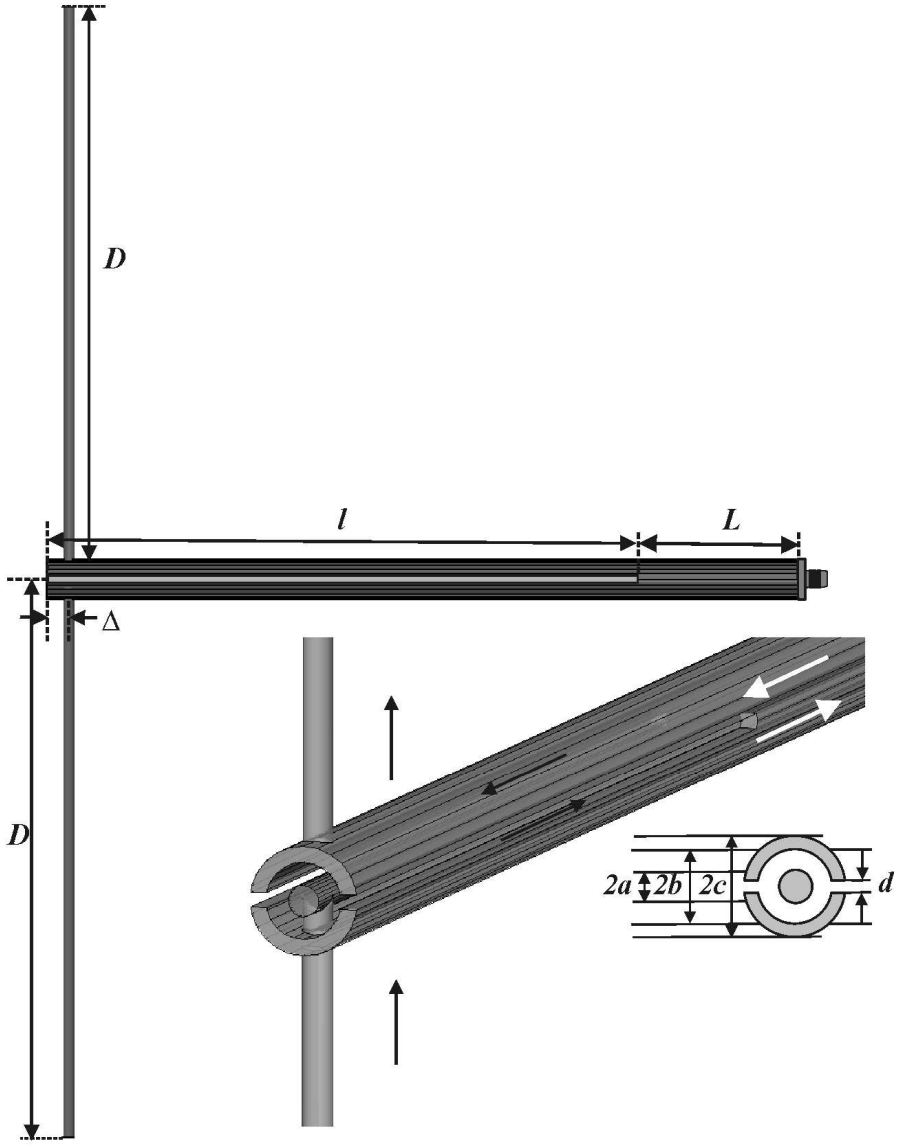

Fig. 1. Split-tube or split-coaxial balun geometry and associated dimensions.

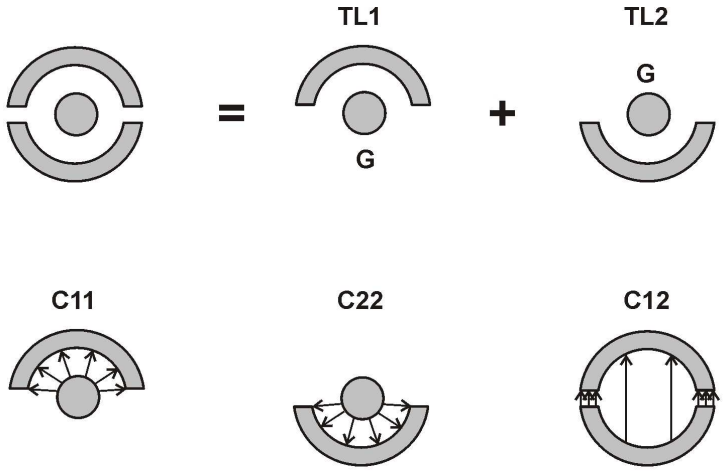

Fig. 2. Top - separation of the splitted coaxial line into two symmetric coupled lines; bottom - static capacitances: self capacitances C_{11} and C_{22}, and mutual capacitance C_{12}.

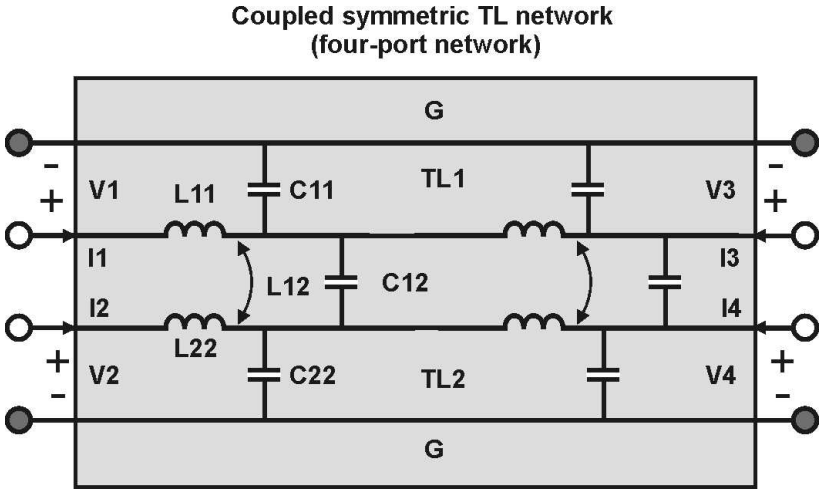

Fig. 3. Coupled symmetric transmission line model of the balun.

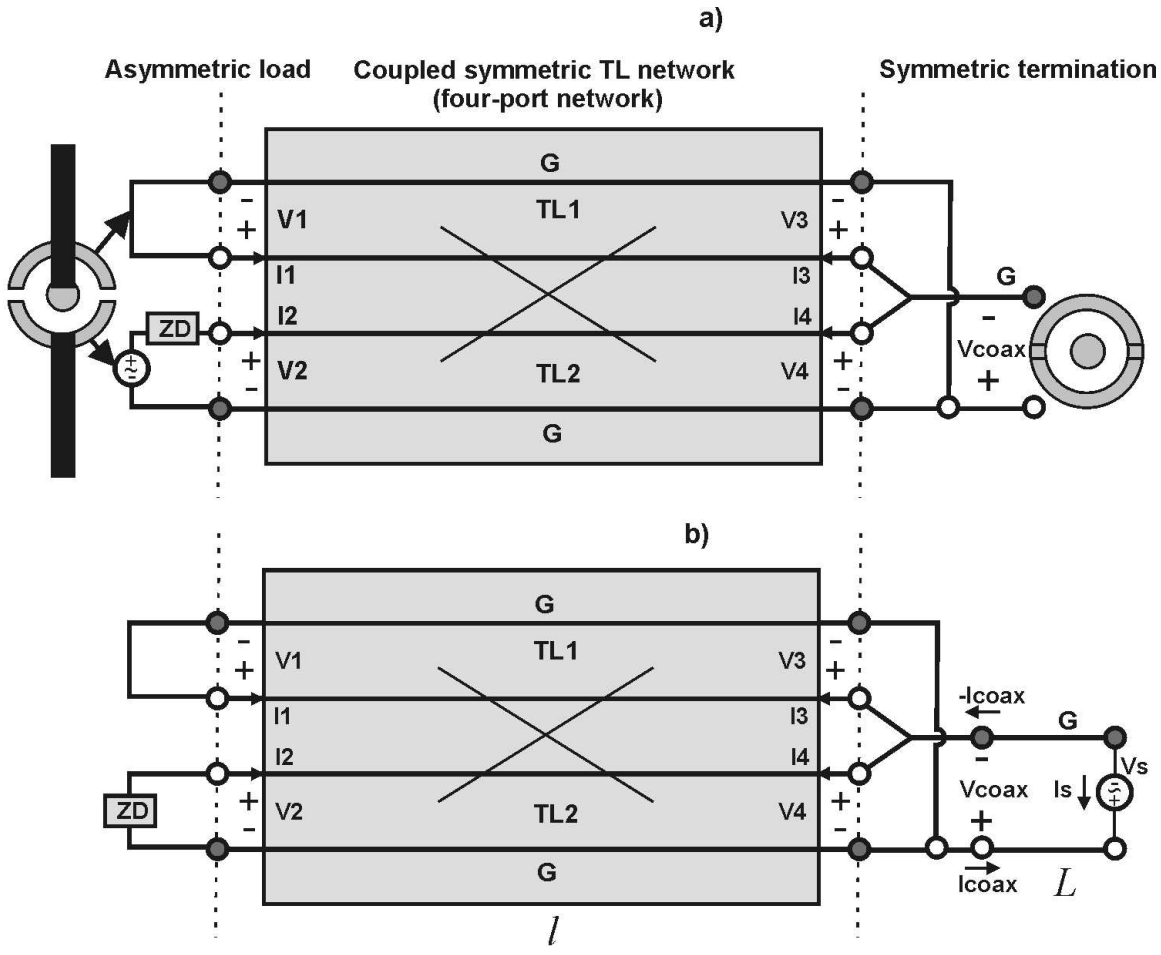

Fig. 4. Two termination schemes: a) - receiving dipole connected to the balun and a coaxial transmission line; b) - termination network used to find the transformed impedance $Z_s = V_s / I_s$ of the dipole with center-fed impedance Z_D connected to a balun of length *l* and a coaxial TL section of length *L*.

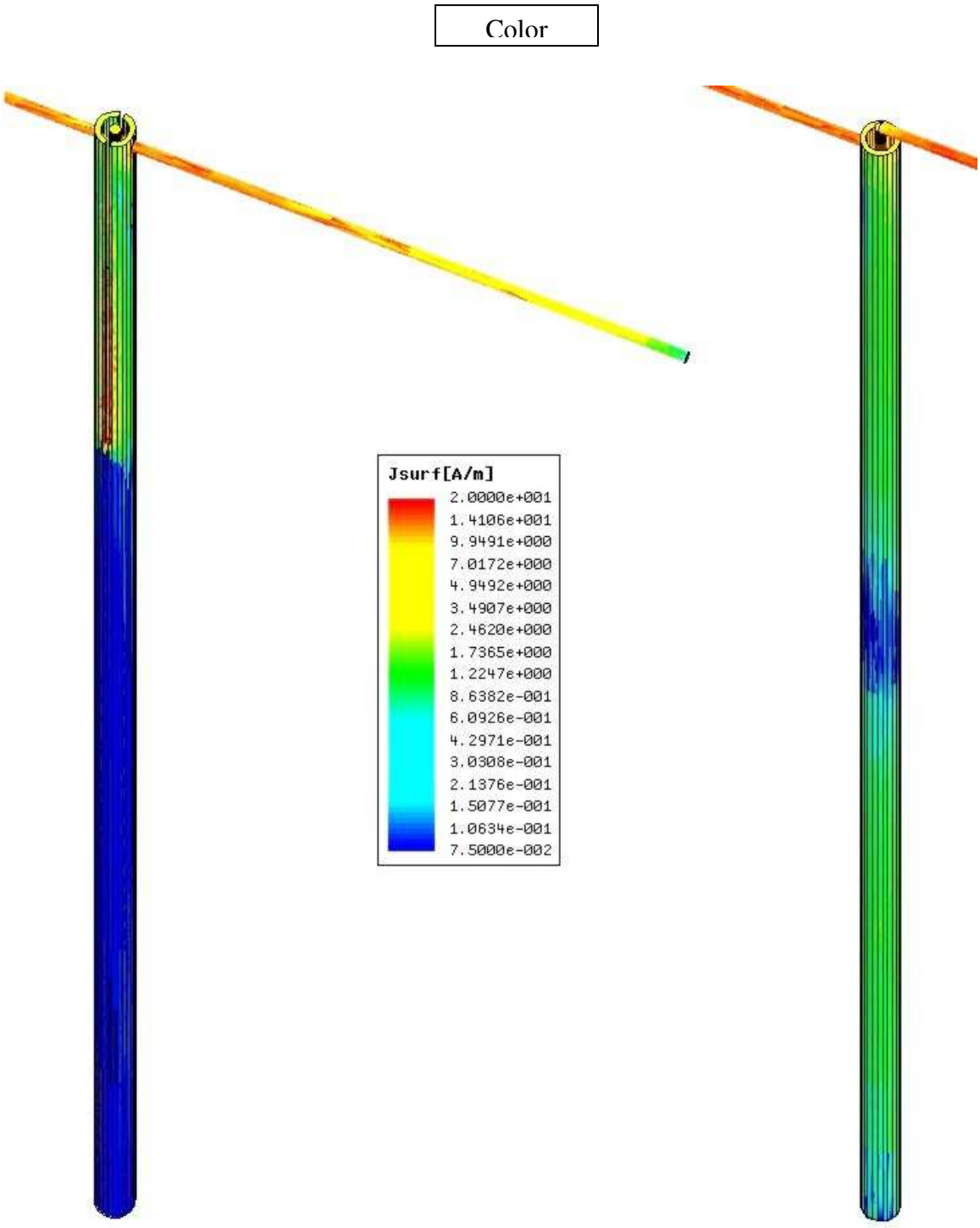

Fig. 5. Surface current density distribution (logarithmic scale) for a dipole with splitted-coaxial balun (left) and for the unbalanced dipole with the same parameters (Table 1)-right.

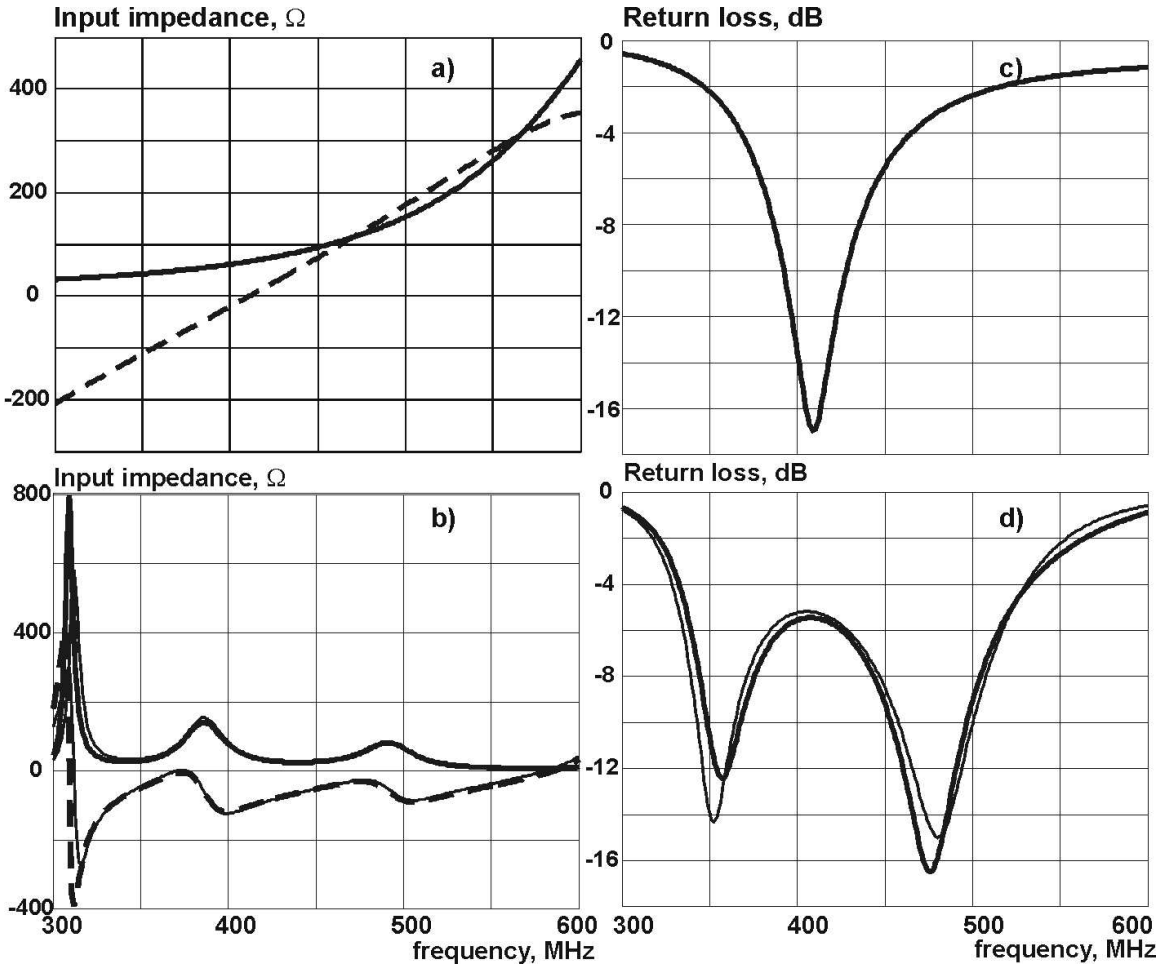

Fig. 6. a) - Impedance behavior of the center-fed test dipole with 170 mm wings; b) - impedance of the same dipole connected to the balun and a continued coaxial line with the characteristic impedance of 54 Ω - see Table 1. Resistance is shown by a solid curve, reactance is shown by a dashed curve. c), d) - Return loss for the cases a) and b), respectively. All solutions are obtained using ANSOFT HFSS. The result of the transmission line theory (Eqs. (12)) is given by thin curves in Fig. 6b) and 6d).

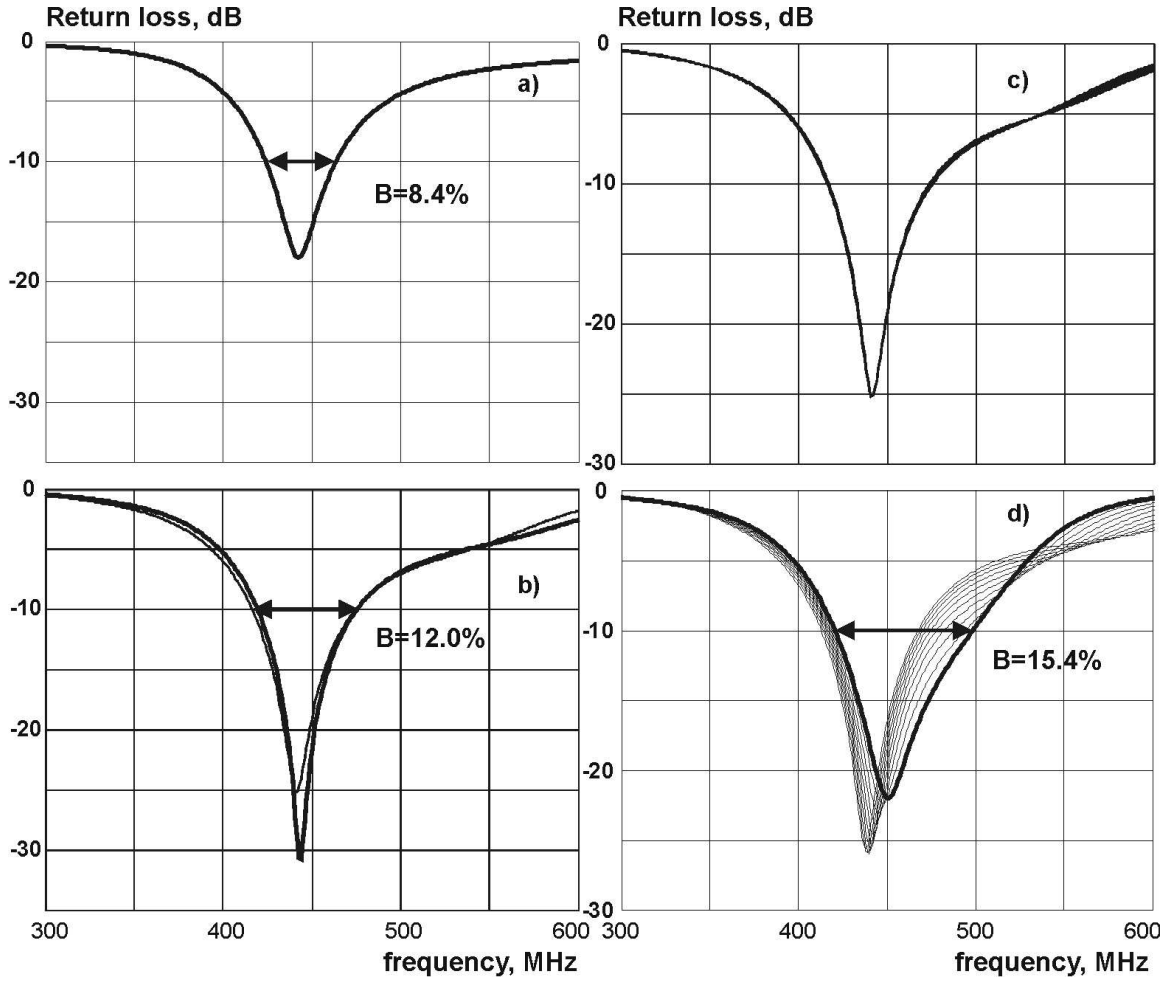

Fig. 7. a) - Return loss of the center-fed dipole with 156 mm wings; b) - return loss of the dipole with balun according to Table 2. Thick curve - ANSOFT HFSS solution; thin curve - transmission line model. c) - effect of varying slot width from 1 to 2 mm on the return loss - transmission line model. d) - effect of varying slot length about $\lambda_{Dres}/4$ by $\pm 10\%$ on the return loss; thick curve corresponds to $\lambda_{Dres}/4+10\%$ - transmission line model.

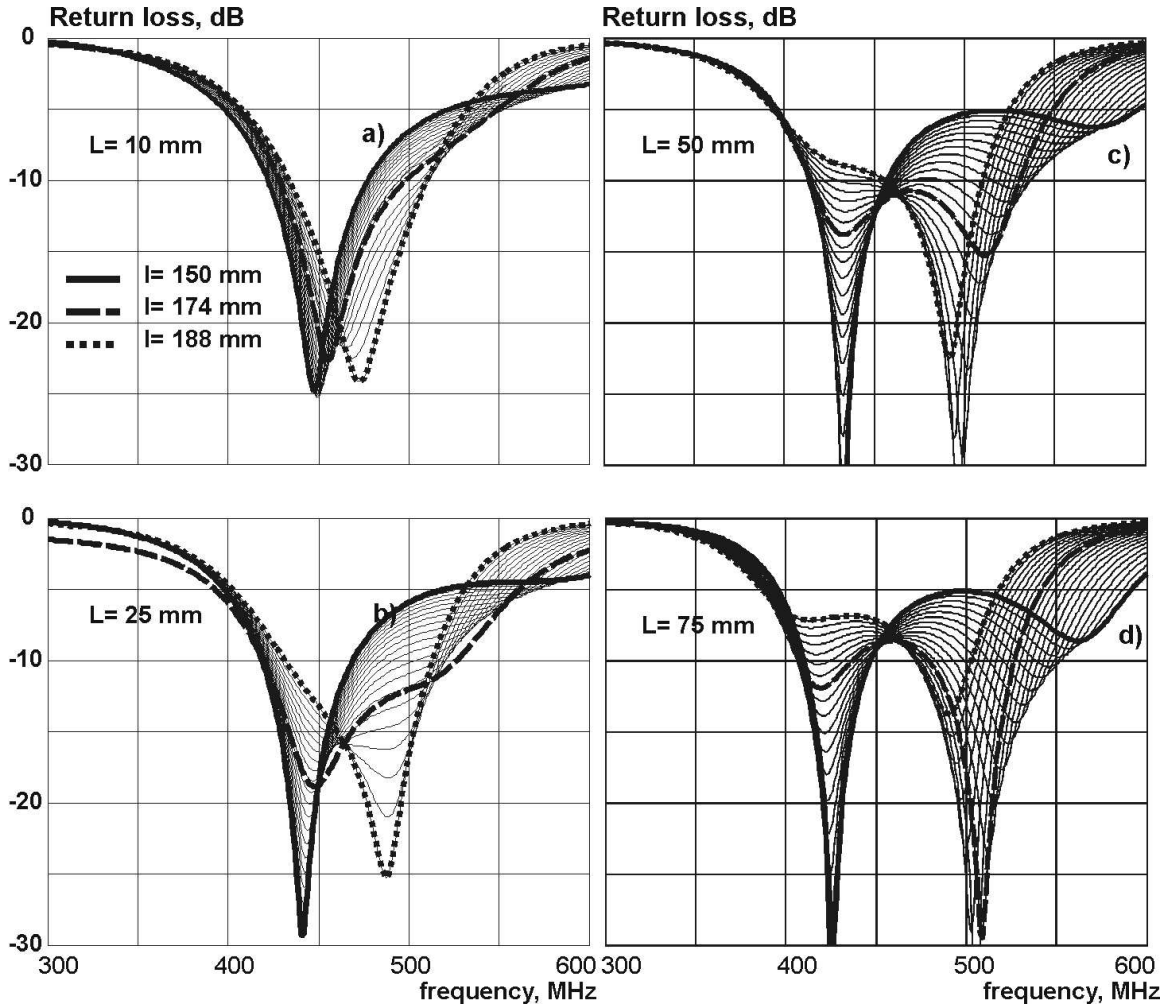

Fig. 8. Development of the second resonance with increasing the length of the non-splitted transmission line section. a) - $L = 10\text{mm}$; b)- $L = 25\text{mm}$; c) - $L = 50\text{mm}$; d) - $L = 75\text{mm}$. In every plot, a sweep is made over the balun length l that varies from 150 to 188mm in 20 uniform steps.

Fig. 9. A series of dipole prototypes built according to data from Table 3.

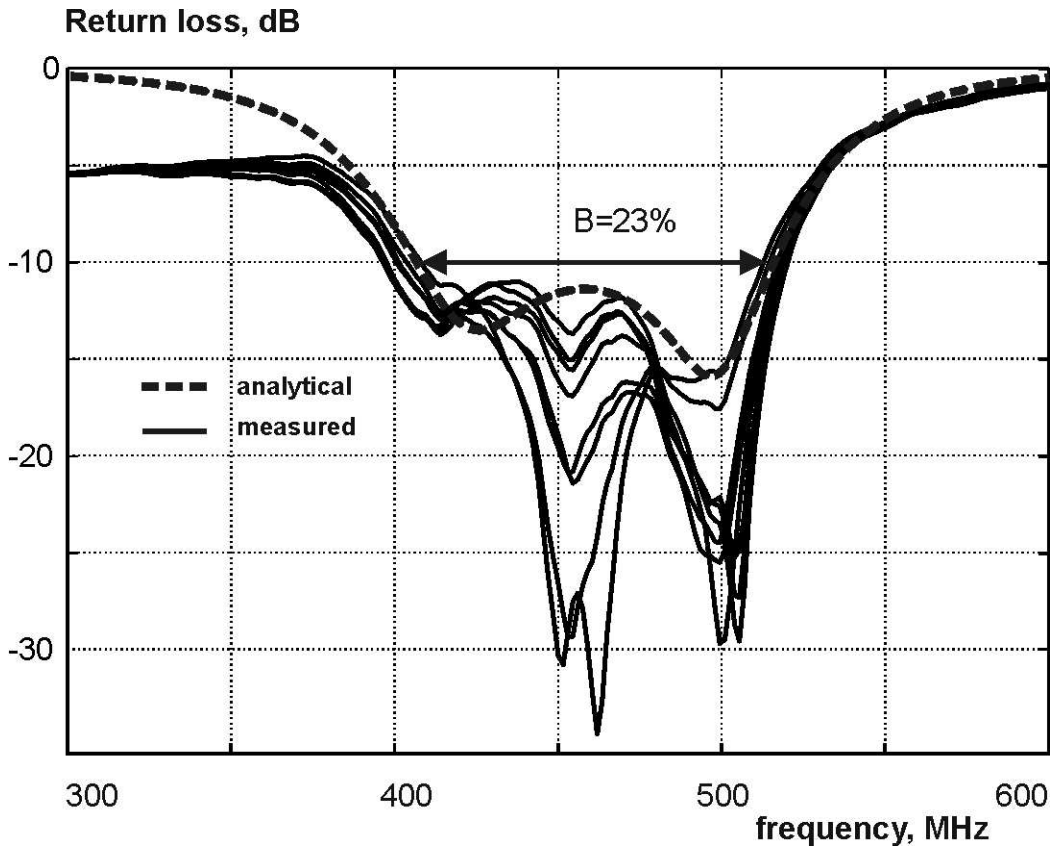

Fig. 10. Return loss measurements for a series of 460 MHz dipoles (thin curves) compared to the corresponding analytical TL solution - thick dashed curve. The minimum experimental 10 dB bandwidth is 23%.

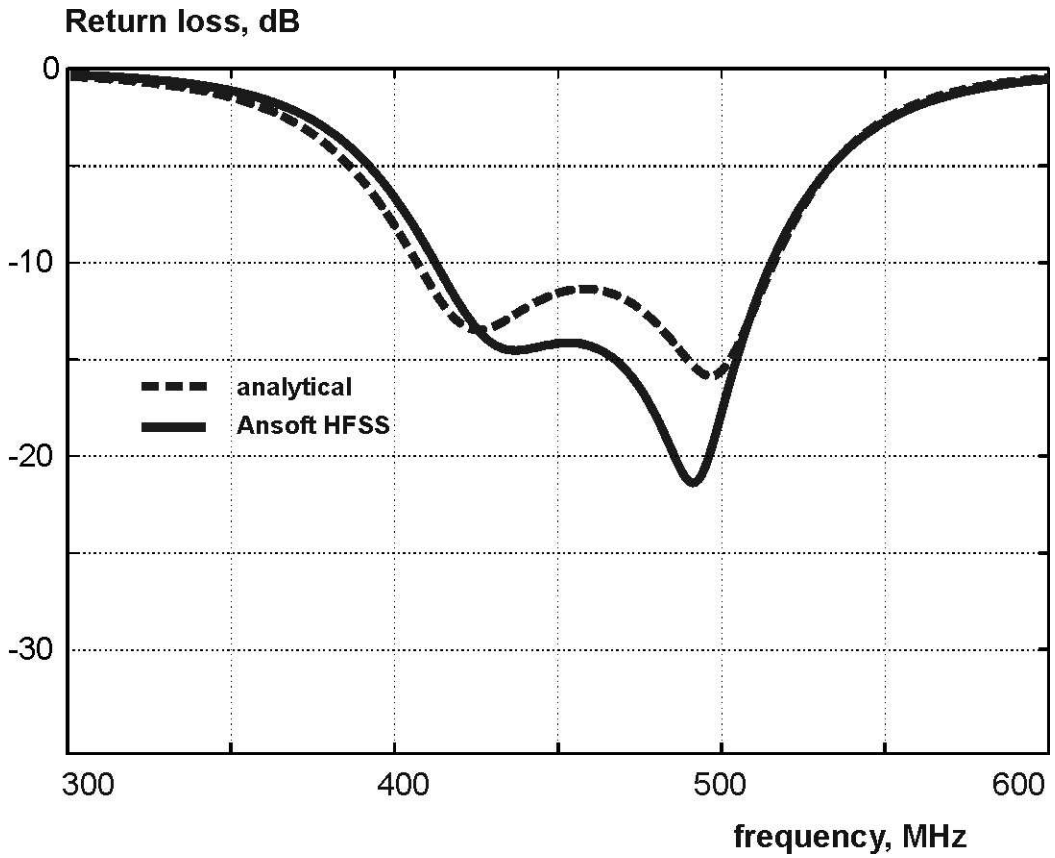

Fig. 11. Analytical TL solution for the dipole prototype vs. the corresponding full-wave ANSOFT HFSS simulation.